Research Article

Oliver Kranz*, Ralf D. Geckeler, Andreas Just, Michael Krause and Wolfgang Osten

From plane to spatial angles: PTB's spatial angle autocollimator calibrator

Abstract: Electronic autocollimators are utilised versatilely for non-contact angle measurements in applications like straightness measurements and profilometry. Yet, no calibration of the angle measurement of an autocollimator has been available when both its measurement axes are engaged. Additionally, autocollimators have been calibrated at fixed distances to the reflector, although its distance may vary during the use of an autocollimator. To extend the calibration capabilities of the Physikalisch-Technische Bundesanstalt (PTB) regarding spatial angles and variable distances, a novel calibration device has been set up: the spatial angle autocollimator calibrator (SAAC). In this paper, its concept and its mechanical realisation will be presented. The focus will be on the system's mathematical modelling and its application in spatial angle calibrations. The model considers the misalignments of the SAAC's components, including the non-orthogonalities of the measurement axes of the autocollimators and of the rotational axes of the tilting unit. It allows us to derive specific measurement procedures to determine the misalignments *in situ* and, in turn, to correct the measurements of the autocollimators. Finally, the realisation and the results of a traceable spatial angle calibration of an autocollimator will be presented. This is the first calibration of this type worldwide.

Keywords: angle metrology; autocollimator calibration; deflectometry; spatial angles; synchrotron metrology.

DOI 10.1515/aot-2015-0017
Received February 23, 2015; accepted April 23, 2015; previously published online May 21, 2015

***Corresponding author: Oliver Kranz,** Physikalisch-Technische Bundesanstalt (PTB), Bundesallee 100, D-38116 Braunschweig, Germany, e-mail: oliver.kranz@ptb.de
Ralf D. Geckeler, Andreas Just and Michael Krause: Physikalisch-Technische Bundesanstalt (PTB), Bundesallee 100, D-38116 Braunschweig, Germany
Wolfgang Osten: Institut für Technische Optik (ITO), Universität Stuttgart, Pfaffenwaldring 9, D-70569 Stuttgart, Germany

www.degruyter.com/aot

1 Introduction

For angle measurements with autocollimators, the most demanding challenges are imposed by their use in deflectometric profilometers [1–3]. These instruments are used for high precision form measurements of optical surfaces where interferometric measurements appear impractical because, e.g., of the size (up to 1.5 m) of the investigated object or its high dynamic topography range. Deflectometric profilometres are used in metrology laboratories of synchrotrons and free electron lasers (FEL) [4, 5] and in national metrology institutes [6]. To determine the surface form, the autocollimator measures the local slope of the surface via a pentaprism or optical square. By moving the pentaprism along the autocollimator's optical axis, the surface is scanned, and its form is reconstructed by an integration of the measured angles. Two important challenges to autocollimator calibrations originate from this working principle: variable distances due to the movement of the pentaprism and the simultaneous engagement of both measurement axes of the autocollimator due to the deflection direction of the reflected beam which is, in a general case, not in the direction of only one of the measurement axes.

High demands are put on the accuracy of those form measurements (2 nm p-v in form, 50 nrad rms in slope [7]) and, therefore, on the characterisation and calibration of the utilised autocollimators. To date, autocollimator calibrations at Physikalisch-Technische Bundesanstalt (PTB) have been performed for plane angles at fixed distances (permissible range: 250–500 mm [8, 9]). A commercial, piezo-driven system for the actuation of a mirror's pitch and yaw angle had been built up at PTB [10]. However, this measurement setup aimed at testing error separation techniques rather than performing calibrations of autocollimators.

To achieve fundamental limits in the autocollimator-based deflectometric form measurement, the calibrations need to be adapted to the prevalent measurement conditions: spatial angles of the mirror, which engage both measurement axes of the autocollimator simultaneously and varying distances between the autocollimator and the mirror. PTB's new calibration device, the spatial angle

autocollimator calibrator (SAAC), offers both. It relies on a Cartesian arrangement of three autocollimators (two calibrated reference autocollimators, one autocollimator to be calibrated), which face a reflector cube. The cube's tilting angles are measured by the reference autocollimators to calculate its angular orientation. These values are compared to the measurements of the autocollimator to be calibrated.

In this paper, the concept and the realisation of the SAAC in PTB's clean-room facility will be outlined. The mathematical model of the SAAC and the derivation of appropriate alignment measurements will be explained in detail. The determination of non-orthogonalities of the optical faces of the reflector cube, of the tilting unit's rotational axes and of the autocollimator's measurement axes will be presented. The last part of this paper will illustrate the spatial angle calibration of an autocollimator, which makes use of the derived alignment parameters. The measurement values of the reference autocollimators are corrected by plane angle calibrations of their respective main measurement axis. We explain how the traceability of the spatial angle calibration to the national standard for the plane angle, the WMT 220 [11], is achieved by means of the Cartesian arrangement. Finally, the experimental result of a spatial calibration of an autocollimator will be presented.

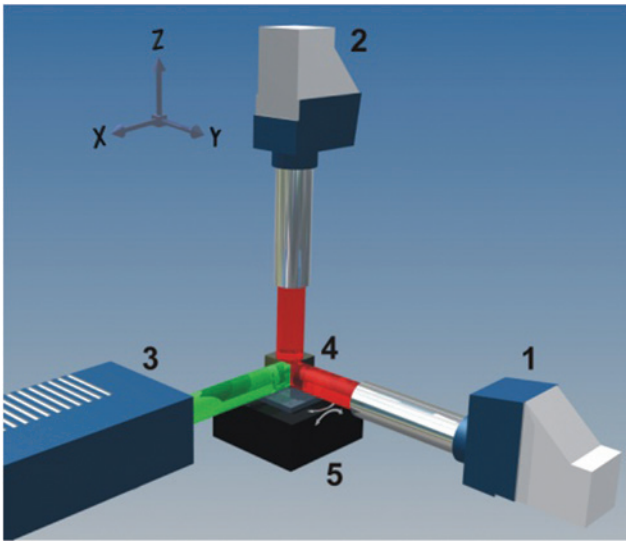

Figure 1: Key components of the SAAC. 1: horizontal reference autocollimator, 2: vertical reference autocollimator, 3: autocollimator to be calibrated, 4: reflector cube, 5: two-axis tilting unit.

2 Concept and realisation of the SAAC

2.1 Cartesian arrangement of the autocollimators and the cube

The SAAC relies on a novel concept, a Cartesian arrangement of three autocollimators which face a reflector cube, which has been developed by PTB [12]. The cube is located on a two-axis tilting unit. Two of the autocollimators serve as reference measurement systems, while the third autocollimator is the autocollimator to be calibrated. See Figure 1 for the basic components and their arrangement in the SAAC.

The Cartesian arrangement of the three autocollimators and the reflector cube is the key concept of the SAAC. As seen from the autocollimator to be calibrated, the tilting unit rotates the cube in pitch and yaw directions to fully cover the autocollimator's horizontal and vertical measurement range. Each reference autocollimator is primarily sensitive to only one of the tilting angles of the cube (horizontal reference autocollimator: yaw angle, vertical reference autocollimator: pitch angle). The advantage of this arrangement will be emphasised in Section 6.

2.2 Mechanical realisation and specifications of the system and its components

A massive granite plate (weight: 3 t, dimensions L×W×H: 2950×850×400 mm^3) and a bridge are the base of the whole SAAC on which all other components are mounted. It is supported by three pairs of vibration isolator legs, which effectively form a three-point carriage. Therefore, the whole structure is unsusceptible to external tremors and, due to the solid granite, to vibrations and resonances. A linear stage (area: 500×500 mm^2) is integrated in the base plate. It bears the autocollimator to be calibrated and allows the variation of the distance to the reflector cube from 200 mm to 1500 mm.

The tilting unit consists of two rotational air bearings (one per axis). Each rotational axis is realised by a closed-loop system of two voice-coil actuators combined with a measurement system, which consists of a radial grating and two reading heads. The pairs of actuators are diametrically opposed to minimise non-radial moments. Both rotational axes have an angular movement range of 6000 arcsec. The two-axis tilting unit and the granite base plate with the bridge and the vibration isolation were custom-made by Q-Sys (Helmond, The Netherlands).

Two autocollimators of the type Elcomat 3000 (by Möller-Wedel Optical, Wedel, Germany, [13]) are used as reference measurement devices. They have been chosen with respect to the provided measurement range in connection with their measurement accuracy (measurement resolution: 0.001 arcsec, calibration uncertainty: <0.005 arcsec [3, 14]). Additionally, PTB has ample expertise regarding this type of autocollimator. The reference autocollimators are mounted on the granite bridge and can be adjusted. They measure the angular orientation of the cube, while the measurement systems of the rotational axes of the tilting unit are used for positioning purposes only.

Two variants of reflector cubes (material: quartz, dimensions: 65×65×65 mm^3) have been manufactured by Carl Zeiss (Jena, Germany). Variant one features two reflective sides and one non-reflective plain side, while variant two has three reflective faces. For both variants, the sides whose angles are measured by the reference autocollimators are reflective. For the autocollimator to be calibrated, high reflectivity or low reflectivity can be chosen as demanded by the customer. The non-orthogonalities of the relevant faces are below 5 arcsec, while their planarity deviations are below 15 nm p-v. The cubes are fastened by adapter plates, which are mounted on the tilting unit. The adapter plates allow a fine adjustment of the alignment of the cube. The pivot point of the cube with respect to the tilting unit is located in its centre, i.e., the unit's rotational axes cross at this point. Figure 2 shows photographs of the SAAC in PTB's clean-room facility. See [12] for an extensive description and technical details of the system.

3 Modelling

3.1 Alignment parameters, vector representation and goal of the modelling

The goal of the mathematical modelling of the SAAC is to enable the calculation of the angle values, which are measured by the autocollimators as a function of all influencing parameters. The mathematical model incorporates the tilting angles of the cube as well as the characteristics of the particular components (non-orthogonalities of the faces of the reflector cube, non-orthogonality of the rotational axes of the tilting unit, non-orthogonality of the measurement axes of the autocollimators) and the relative angular orientations of all components. All these variables are called alignment parameters in this document.

The autocollimators' beams and measurement axes, the cube's surfaces' normals and the rotational axes of the tilting unit are represented as vectors given in a global reference coordinate system. Figure 3 shows the ideal (error-free) orientation of the components where all vectors are parallel to one of the coordinate axes.

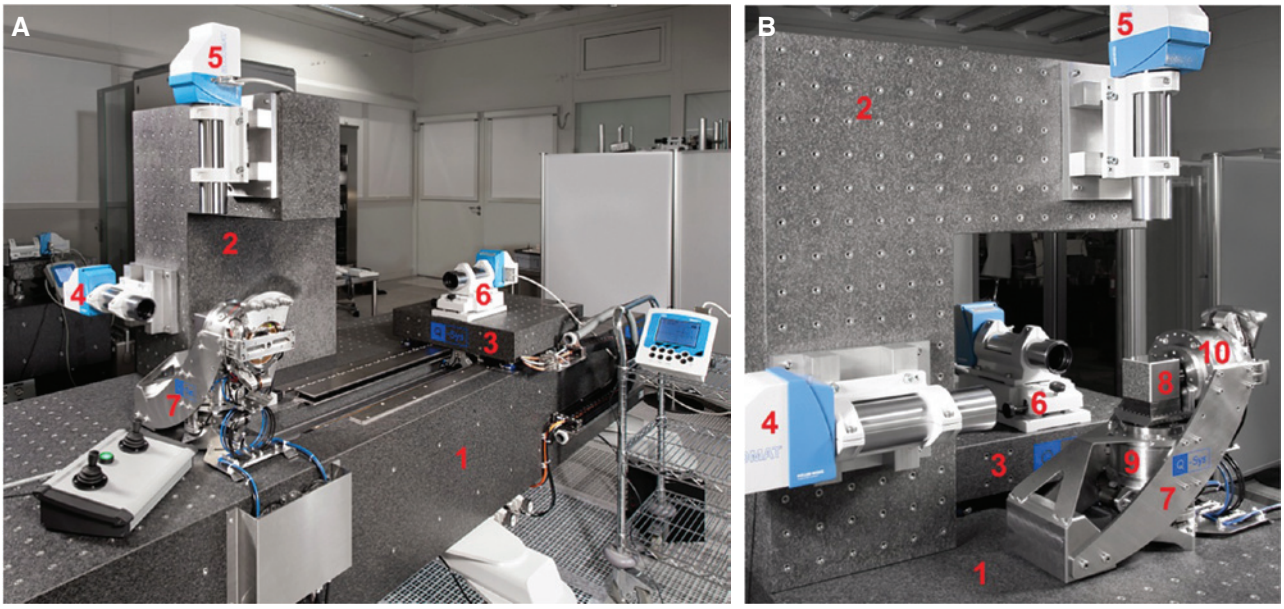

Figure 2: The SAAC in PTB's clean-room facility. Side-view of the SAAC (A). 1: granite base plate, 2: granite bridge, 3: linear stage, 4: horizontal reference autocollimator, 5: vertical reference autocollimator, 6: autocollimator to be calibrated, 7: two-axis tilting unit. Front-view of the SAAC showing details of the tilting unit (B). 8: cube, 9: air bearing for horizontal tilting, 10: air bearing for vertical tilting.

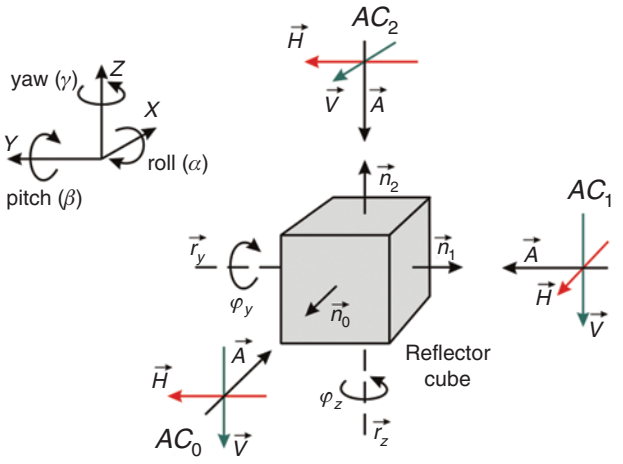

Figure 3: Initial orientation of the SAAC components, represented as vectors. The reference coordinate system is shown in the upper left corner. AC_0, AC_1, AC_2: autocollimator to be calibrated, horizontal reference autocollimator, and vertical reference autocollimator. $\vec{H}$, $\vec{V}$, $\vec{A}$: horizontal measurement axis, vertical measurement axis and optical axis of each autocollimator. $\vec{n}_0$, $\vec{n}_1$, $\vec{n}_2$: surfaces of the reflector cube. $\vec{r}_y$, $\vec{r}_z$: rotational axes of the tilting unit. φ_y, φ_z: tilting angles of the cube with respect to the rotational axes.

The SAAC ray-tracing model comprises the following alignment parameters:

- angular orientations of the autocollimators (three per autocollimator AC_i: $AC_{i\alpha}$, $AC_{i\beta}$, $AC_{i\gamma}$, i={0, 1, 2} in total nine)
- non-orthogonalities of the autocollimators' measurement axes (1 per AC_i: V_{iv}, in total three)
- initial angular orientation of the cube relative to the tilting unit (three: W_α, W_β, W_γ)
- orthogonality deviations of the cube's optical surfaces (three: $n_{0\beta}$, $n_{0\gamma}$, $n_{2\alpha}$)
- orthogonality deviation of the tilting unit's rotational axes ($r_{y\alpha}$)
- tilting angles of the cube with respect to the tilting unit's rotational axes (two: φ_y, φ_z).

The parameters indicate, in which way the corresponding components are misaligned. They are defined as rotational angles acting on vectors in the ideal (un-rotated) alignment state presented in Figure 3. They are given as angular values for the rotations around the reference coordinate system's axes. α denotes a rotation around the x-axis, β denotes a rotation around the y-axis and γ denotes a rotation around the z-axis. The non-orthogonalities of the autocollimators' measurement axes (V_{0v}, V_{1v}, V_{2v}) are measured as clockwise rotations around the optical axes of the autocollimators.

In this consideration, the orientation of the reference coordinate system is defined by the rotational axes $\vec{r}_y$ and $\vec{r}_z$ of the tilting unit (for the unit's 'zero' position, $\varphi_y=\varphi_z=0$) as follows:

$$\vec{r}_z \| \hat{z} \tag{1a}$$

$$\vec{r}_y \times \vec{r}_z \| \hat{x} \Rightarrow r_{y\alpha} \neq 0 \tag{1b}$$

where $r_{y\alpha}$ is the non-orthogonality of $\vec{r}_y$ and $\vec{r}_z$.

The vertical rotational axis, $\vec{r}_z$, is parallel to the z-axis of the global coordinate system, while the horizontal rotational axis, $\vec{r}_y$, lies in the y-z plane. The resulting vector, which is formed by the cross product of $\vec{r}_y$ and $\vec{r}_z$, is parallel to the x-axis of the global coordinate system (see Figure 3).

For the tilting unit's 'zero' position ($\varphi_y=\varphi_z=0$) and an ideal alignment of the cube with respect to the tilting unit, $W_\alpha=W_\beta=W_\gamma=0$, the angular orientation of the cube with respect to the global coordinate system can be defined by the surface normals $\vec{n}_1$ and $\vec{n}_2$ with

$$\vec{n}_1 \| \hat{y} \tag{2a}$$

$$\vec{n}_1 \times \vec{n}_2 \| \hat{x} \Rightarrow n_{2\alpha} \neq 0 \tag{2b}$$

The surface normal $\vec{n}_1$ is parallel to the y-axis of the global coordinate system. $\vec{n}_2$ lies in the y-z plane. The vector, which is formed by the cross product of $\vec{n}_1$ and $\vec{n}_2$, is parallel to the x-axis of the global coordinate system. The remaining alignment parameters, $n_{0\beta}$, $n_{0\gamma}$ and $n_{2\alpha}$, are derived from the orthogonality deviations between two of the three relevant surface normals, respectively (see Section 5.1). Owing to the choice of the cube's reference alignment (2a,b), $\vec{n}_1$ has no orthogonality deviation, and $\vec{n}_2$ only has one. Still, the surface normals' orthogonality deviations cover all dimensions of the global coordinate system.

The model fulfils two purposes. First, the autocollimators' measurement values are influenced by the alignment parameters. With the help of the model, the alignment parameters can be determined by appropriate measurement procedures, which are derived from the model equations (see Section 4.3). Additionally, these measurements can be used to improve the adjustment of the system's components after assembly.

Second, for the spatial angle calibration of the autocollimator to be calibrated, the tilting angles of the cube need to be determined. As the alignment parameters affect the autocollimators' measurement values, the angles of the cube are not directly accessible. Therefore, they are calculated by an optimisation algorithm, which makes use of the measurement values of the reference

autocollimators in addition to the predetermined alignment parameters (see Section 6). With the alignment parameters of the autocollimator to be calibrated and the tilting angles of the cube, the angle deviations (difference between measurement value and geometric angle) of this autocollimator can be determined.

Both applications of the mathematical model of the SAAC, the determination of alignment parameters and the calculation of the cube's tilting angles, will be explained in detail.

3.2 Autocollimator beam ray tracing and polynomial approximations

To obtain the measurement values of the autocollimators, their beams are emitted along their optical axes and reflected at the respective surfaces of the reflector cube. Then, the reflected beams' orientations in the autocollimators' local coordinate systems are regarded. The resulting measurement values are determined by calculating the deflection angles of the reflected beam in the directions of the measurement axes of the autocollimators. It should be noted that the autocollimators do not measure polar coordinates of the reflecting surfaces, but rather two independent deflection angles in the directions of their measurement axes. Therefore, both measurement axes are treated separately for each autocollimator. For a detailed review of the characteristics of spatial angle deflections, the ray tracing of the autocollimator beams, the calculation of the autocollimators' measurement values and their relation to the polar coordinates of the reflecting surface, see [12] and [15].

Owing to an initial alignment, all components' angular alignment deviations from the ideal alignment are supposed to be <100 arcsec. The surfaces' non-orthogonalities are of the order of a few arcseconds. The non-orthogonalities of the tilting unit's rotational axes and of the autocollimators' measurement axes are, furthermore, of the order of a few 10 arcsec. Therefore, the exact but complex model can be simplified by approximating the multiply nested trigonometric functions with polynomial expressions. The absolute angle difference between the exact model and the approximated model is $<10^{-3}$ arcsec.

Two sets of polynomial formulas have been created:

- A set of equations, which covers all terms that contribute to the measurement values at excess of 10^{-4} arcsec for the tilting angles of the cube (φ_y, φ_z) being in a range of ±2000 arcsec. Therefore, first-, second- and third-order terms occur. Note that the calibration range of the SAAC is limited by the measurement range of the utilised reference autocollimators to ±1500 arcsec per measurement axis.
- A simplified set of equations, which identifies the alignment parameters of the SAAC that introduce first- and second-order terms to the measurements of the autocollimators. These equations will be used to derive and evaluate alignment measurements for the determination of the adjustment of the SAAC's components.

With the definitions of the global coordinate system [equations (1)] and the orientation of the cube for an ideal alignment with respect to the tilting unit [equations (2)], the polynomial functions for the measurement values of the autocollimators are given by:

$$\begin{aligned} H_0 = &-\varphi_z + \varphi_y(AC_{0\alpha} - r_{y\alpha}) - W_\gamma - n_{0\gamma} + AC_{0\gamma} \\ &+ AC_{0\alpha}(W_\beta - AC_{0\beta} + n_{0\beta}) - n_{0\beta}W_\alpha \end{aligned} \tag{3a}$$

$$\begin{aligned} V_0 = &-\varphi_y + \varphi_z(-V_{0\nu} - AC_{0\alpha}) - W_\beta - n_{0\beta} + AC_{0\beta} \\ &+ AC_{0\alpha}(AC_{0\gamma} - W_\gamma - n_{0\gamma}) + V_{0\nu}(AC_{0\gamma} - W_\gamma - n_{0\gamma}) + n_{0\gamma}W_\alpha \end{aligned} \tag{3b}$$

$$H_1 = -\varphi_z + \varphi_y(W_\alpha - r_{y\alpha}) - W_\gamma + AC_{1\gamma} - AC_{1\beta}W_\alpha + W_\alpha W_\beta \tag{3c}$$

$$\begin{aligned} V_1 = &\varphi_z(-V_{1\nu} - AC_{1\beta}) + \varphi_y W_\gamma + W_\alpha - AC_{1\alpha} \\ &+ AC_{1\beta}(AC_{1\gamma} - W_\gamma) + V_{1\nu}(AC_{1\gamma} - W_\gamma) \end{aligned} \tag{3d}$$

$$H_2 = \varphi_y(\varphi_z - AC_{2\gamma}) + \varphi_z W_\beta - W_\alpha - n_{2\alpha} + AC_{2\alpha} - AC_{2\gamma}W_\beta + W_\beta W_\gamma \tag{3e}$$

$$\begin{aligned} V_2 = &-\varphi_y + \varphi_z(-n_{2\alpha} - W_\alpha) - W_\beta + AC_{2\beta} \\ &+ AC_{2\gamma}(W_\alpha + n_{2\alpha}) + V_{2\nu}(AC_{2\alpha} - W_\alpha - n_{2\alpha}) - W_\alpha W_\gamma - n_{2\alpha}W_\gamma \end{aligned} \tag{3f}$$

For an error-free alignment of the components (all alignment parameters are zero), the measurement values of the three autocollimators appear as shown in Figure 4 for a 1800×1800 arcsec² calibration grid of 19×19 measurement positions.

3.3 Derivation of alignment measurements

In this section, we derive measurement strategies, which enable us to determine the alignment parameters of the cube (W_α, W_β, W_γ) and of the autocollimators ($AC_{0\alpha}$, $AC_{0\beta}$, $AC_{0\gamma}$, $AC_{1\alpha}$, $AC_{1\beta}$, $AC_{1\gamma}$, $AC_{2\alpha}$, $AC_{2\beta}$, $AC_{2\gamma}$) by the use of the polynomial equations (3). For clarity, in this document, the expressions for the horizontal and vertical measurement values of the autocollimators are represented by $H_i(\varphi_y, \varphi_z)$ and $V_i(\varphi_y, \varphi_z)$, $i \in \{0, 1, 2\}$. The non-orthogonalities of the

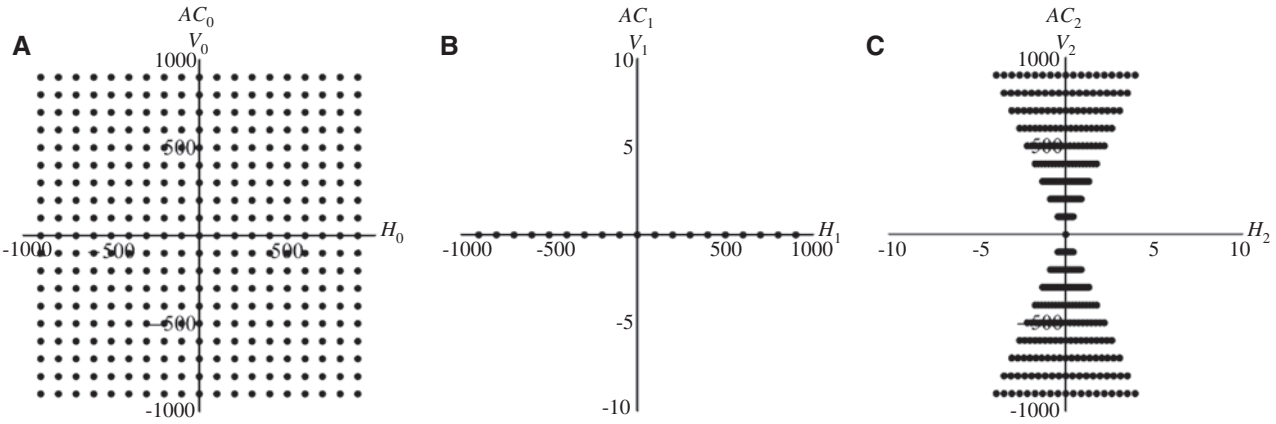

Figure 4: Angular response of AC_0, the autocollimator to be calibrated (A), AC_1, the horizontal (B) and AC_2, the vertical reference autocollimator (C) for a calibration grid of 1800×1800 arcsec². Notice the different scaling of the axes in the case of (B) and (C); the two reference autocollimators are primarily sensitive to only one of the cube's tilting angles, while the autocollimator to be calibrated is sensitive to both.

measurement axes of the autocollimators, $V_{0\nu}$, $V_{1\nu}$ and $V_{2\nu}$, the non-orthogonality of the rotational axes of the tilting unit, $r_{y\alpha}$, and the non-orthogonalities of the optical faces of the cube, $n_{0\beta}$, $n_{0\gamma}$, and $n_{2\alpha}$, will be identified by supplementary measurements, which are illustrated in the following section.

Practically, two measurements need to be performed: a *yaw test* (φ_z-tilting of the cube with respect to the vertical rotational axis of the tilting unit, $\vec{r}_z$, while φ_y=0) and a *pitch test* (φ_y-tilting with respect to the horizontal rotational axis, $\vec{r}_y$, while φ_z=0). Additionally, the 'zero' angular orientation of the cube is defined by $\varphi_y=\varphi_z=0$ with the respective measurement values of the autocollimators $H_0(0,0)$, $V_0(0,0)$, $H_1(0,0)$, $V_1(0,0)$, $H_2(0,0)$, $V_2(0,0)$.

3.3.1 Yaw test

For the yaw test, the cube is tilted with respect to the tilting unit's vertical rotational axis, $\vec{r}_z$, while φ_y=0. For the evaluation of the tests, not φ_y and φ_z, but the horizontal and vertical measurement values of the autocollimators are utilised. The measurement values of the autocollimators are expressed as functions of other autocollimator measurement values, e.g., $V_2(H_1)$. The slopes of these linear functions are calculated and yield the alignment parameters. The approach of relying on the autocollimators' measurement values for the determination of the alignment parameters is a great advantage as the tilting angles of the cube, φ_y and φ_z, are not easily accessible. It is similar to the method presented in [16, 17] for determining the alignment of a pentaprism used in an autocollimator-based deflectometric profilometre.

Making use of the yaw test in the SAAC, we obtain the following relations:

$$\frac{\partial V_2}{\partial H_1}=\frac{\partial V_2}{\partial \varphi_z}\left(\frac{\partial H_1}{\partial \varphi_z}\right)^{-1}=W_\alpha+n_{2\alpha} \tag{4a}$$

$$\frac{\partial H_2}{\partial H_1}=\frac{\partial H_2}{\partial \varphi_z}\left(\frac{\partial H_1}{\partial \varphi_z}\right)^{-1}=-W_\beta \tag{4b}$$

$$\frac{\partial V_0}{\partial H_1}=\frac{\partial V_0}{\partial \varphi_z}\left(\frac{\partial H_1}{\partial \varphi_z}\right)^{-1}=AC_{0\alpha}+V_{0\nu} \tag{4c}$$

$$\frac{\partial V_1}{\partial H_1}=\frac{\partial V_1}{\partial \varphi_z}\left(\frac{\partial H_1}{\partial \varphi_z}\right)^{-1}=AC_{1\beta}+V_{1\nu} \tag{4d}$$

3.3.2 Pitch test

For the pitch test, the cube is tilted with respect to the horizontal rotational axis of the tilting unit, $\vec{r}_y$, while φ_z=0. We obtain the relations

$$\frac{\partial V_1}{\partial V_2}=\frac{\partial V_1}{\partial \varphi_y}\left(\frac{\partial V_2}{\partial \varphi_y}\right)^{-1}=-W_\gamma \tag{5a}$$

$$\frac{\partial H_2}{\partial V_2}=\frac{\partial H_2}{\partial \varphi_y}\left(\frac{\partial V_2}{\partial \varphi_y}\right)^{-1}=AC_{2\gamma} \tag{5b}$$

The pitch angles, $AC_{0\beta}$, $AC_{1\alpha}$, $AC_{2\beta}$, and yaw angles, $AC_{0\gamma}$, $AC_{1\gamma}$, $AC_{2\alpha}$, of the autocollimators can be calculated from equations (3) as follows:

$$AC_{0\gamma}=H_0(0,0)+W_\gamma+n_{0\gamma} \quad (6a)$$

$$AC_{1\gamma}=H_1(0,0)+W_\gamma \quad (6b)$$

$$AC_{2\alpha}=H_2(0,0)+W_\alpha+n_{2\alpha} \quad (6c)$$

For the cube's 'zero' angular orientation, $\varphi_y=\varphi_z=0$, we obtain the additional relations

$$AC_{0\beta}=V_0(0,0)+W_\beta+n_{0\beta} \quad (6d)$$

$$AC_{1\alpha}=-V_1(0,0)+W_\alpha \quad (6e)$$

$$AC_{2\beta}=V_2(0,0)+W_\beta \quad (6f)$$

The equations have been simplified as the mixed terms (second-order effects) can be neglected regarding the measurement and correction of the system's alignment errors due to the small angles, which are involved. Monte Carlo simulations showed that the determination of the parameters is limited by the autocollimators' measurement uncertainties.

4 Determination of non-orthogonalities

The non-orthogonalities of the cube's surfaces ($n_{0\beta}$, $n_{0\gamma}$, $n_{1\gamma}$, $n_{1\alpha}$, $n_{2\alpha}$, $n_{1\beta}$), of the measurement axes of the autocollimators (V_{0v}, V_{1v}, V_{2v}), and of the axes of the two-axis tilting unit ($r_{y\alpha}$) affect the autocollimators' measurements [see equation (3)]. Their values are required for the evaluation of the alignment measurements, to correct the calculation of the tilting angles of the cube, and thus, for the calibration of the autocollimator.

4.1 Non-orthogonality of the cube's surfaces

Each of the reflector cube's surfaces is represented by its normal, $\vec{n}_0$, $\vec{n}_1$ and $\vec{n}_2$ (see Figure 3). The relative orientation of the surfaces' normals is defined by the three angles between each pair of normals (see [18] for a general description of the measurement principle). By measuring these angles, the orientation of the normals can be determined and enables the calculation of the three non-orthogonalities $n_{0\beta}$, $n_{0\gamma}$ and $n_{2\alpha}$. The derivation of the required formulas is straightforward and omitted in this document. For the cube that was used during the measurements presented in this document, the following non-orthogonalities have been derived: $n_{0\beta}$=2.42 arcsec, $n_{0\gamma}$=2.98 arcsec and $n_{2\alpha}$=3.42 arcsec.

4.2 Non-orthogonalities of the measurement axes of the autocollimators and the rotational axes of the tilting unit

The characterisation of the non-orthogonalities of the measurement axes of the autocollimators and the rotational axes of the tilting unit can be performed by measurements, which solely rely on the use of the tilting unit and the autocollimator. No external measurement system is required. For these measurements, the horizontal (yaw) and the vertical tilting angles (pitch) of the mirror as seen from the autocollimator are regarded.

The method is based on two different roll angle adjustments of the autocollimator with respect to the tilting unit, which differ by approximately 90°, while two measurements need to be performed per adjustment. The angle between the mirror's horizontal tilting direction and its vertical tilting direction as measured by the autocollimator is given by the sum of the non-orthogonalities for one roll angle adjustment and by the difference of the non-orthogonalities for the other roll angle adjustment. This allows the separation of the non-orthogonalities. The alignment of the CCD lines is regarded to be exact, as their non-orthogonality only introduces a second-order effect to all measurements, which is neglected here. The measurement strategy is thoroughly elucidated in the Appendix.

The measurements were repeatedly performed with four different autocollimators and the tilting unit with additional roll angle adjustments of the autocollimators of 180° and 270° to reduce the error in the determination of the non-orthogonalities.

The non-orthogonalities that were measured for all autocollimators are within the range of -4 to 55 arcsec with standard deviations of the mean values of 0.5...1.3 arcsec. The mean value of the non-orthogonality of the tilting unit's rotational axes is $r_{y\alpha}$=41 arcsec (standard deviation of the mean: 1.1 arcsec).

5 Spatial angle calibration of an autocollimator – experimental data

5.1 Calibration grid

For the extension of the plane angle autocollimator calibrations – where only one of the measurement axes is engaged at a time – to a spatial angle characterisation, the selected measurement positions are extended from a

straight line along one of the autocollimator's measurement axes to a grid. Thereby, both measurement axes of the autocollimator are engaged simultaneously, and their crosstalk can be calibrated.

Spatial angle calibrations of an autocollimator were performed during the commissioning phase of the whole system. A grid of 19×19 measurement positions with a step size of 100 arcsec and a grid of 37×37 measurement positions with a step size of 10 arcsec was used. The analysis of the 19×19 pattern is presented in detail, whereas for the 37×37 pattern, only the resulting angle deviations are presented. The measurements cover ranges of 1800×1800 arcsec^2 and 360×360 arcsec^2, respectively, for the autocollimator to be calibrated (-900 to 900 arcsec and -180 to 180 arcsec for both measurement axes). One complete measurement cycle (which includes moving the cube to all measurement positions and acquiring measurement data for 5 s at each position) takes about 35 min for the 19×19 pattern and 140 min for the 37×37 pattern.

Figure 5 shows the measurement values of the autocollimator to be calibrated (A) and the two reference autocollimators, the horizontal (B) and vertical (C). Regarding the measurement values of the reference autocollimators, only one of their respective measurement axes is engaged primarily, while the measurement values of the orthogonal axes are limited to a small range (AC_1: 0.7 arcsec p-v, AC_2: 8.4 arcsec p-v). Therefore, the measurement values of the reference autocollimators can be corrected with the calibration data obtained from the plane-angle calibrations of their measurement axes. In [8], an extensive description of the calibration of autocollimators at PTB can be found.

By determining the cube's spatial angle with two plane-angle measurements, which are performed by the calibrated reference autocollimators, the whole calibration is traced back to PTB's primary angle standard WMT 220, which is the national standard for the plane angle. In this context, 'traceability of measurands' refers to the metrological concept, which is defined by the *International Vocabulary of Metrology* as the 'property of a measurement result whereby the result can be related to a reference through a documented unbroken chain of calibrations, each contributing to the measurement uncertainty' [19].

5.2 Obtaining the alignment parameters

The derivatives of the autocollimators' measurement values [equations (4) and (5)] have been introduced, and two procedures, called *pitch test* and *yaw test*, were presented. These tests are now used to identify six alignment parameters of the cube and the autocollimators: W_α, W_β, W_γ, which are the orientations of the cube relative to the tilting unit, and $AC_{0\alpha}$, $AC_{1\beta}$, $AC_{2\gamma}$, which are the roll angles of the autocollimators.

For this purpose, the measurement values of the autocollimators, which are related to the pitch and yaw tests (φ_y=0 for the pitch test, φ_z=0 for the yaw test), are extracted from the calibration grid. Selected pairs of these measurement values are assigned to each other (Figure 6). The derivatives were calculated by fitting the pairs of measurement values with linear equations, which are depicted by the straight lines in the figure. The slopes of the straight lines correspond to the derivatives.

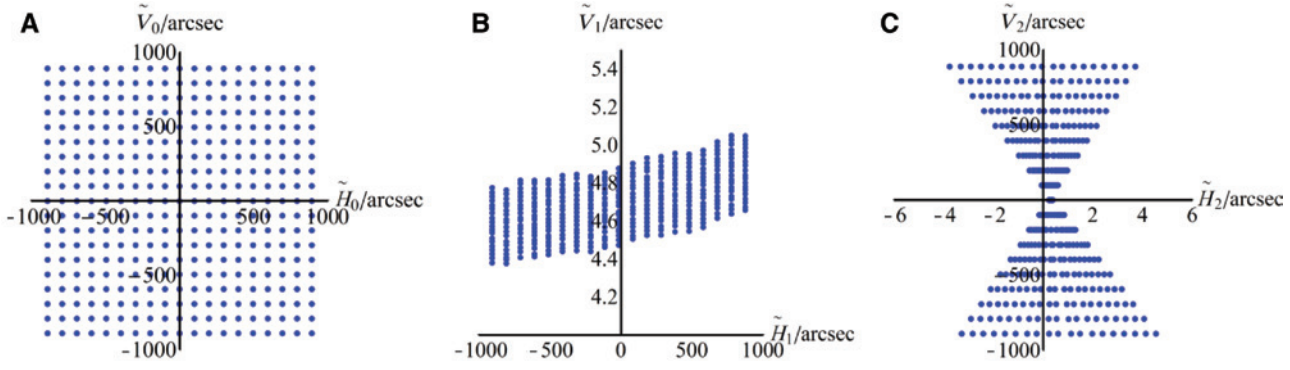

Figure 5: Measurement values of AC_0, the autocollimator to be calibrated (A), AC_1, the horizontal (B) and AC_2, the vertical reference autocollimator (C) in a grid of 19×19 angular positions. The measurement values of the reference autocollimators have been corrected by the respective plane angle calibration data. Note the scaling of the axes; both measurement axes of the autocollimator to be calibrated are engaged, while the reference autocollimators are primarily sensitive to only one of the cube's tilting angles (horizontal reference autocollimator: yaw angle, vertical reference autocollimator: pitch angle).

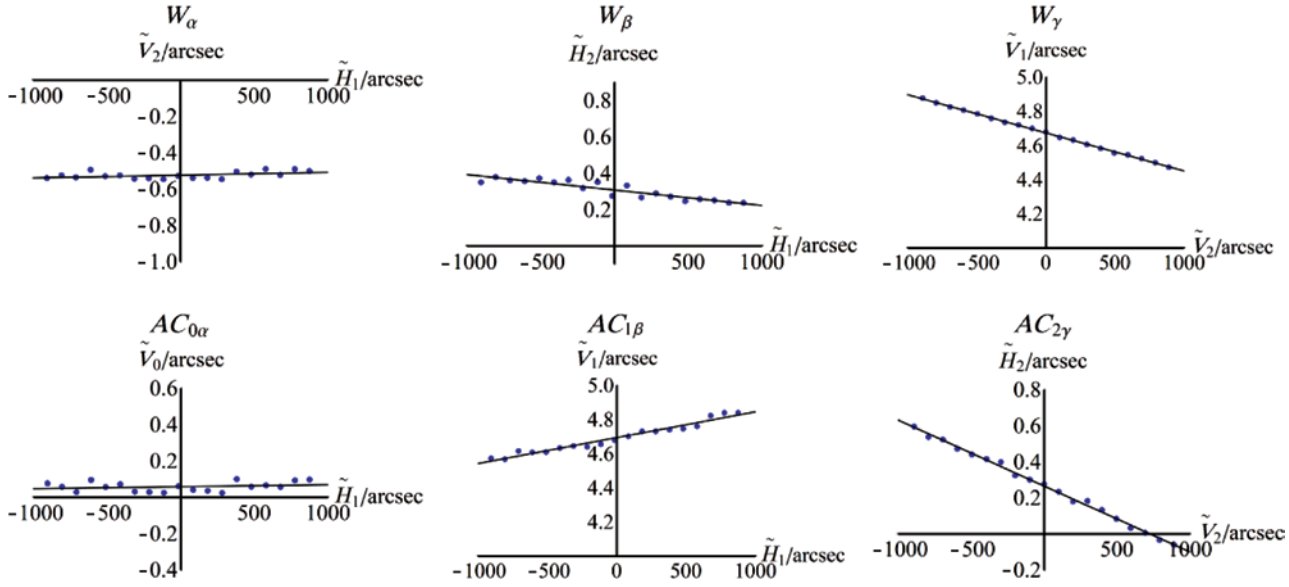

Figure 6: The measurement values of selected pairs of the autocollimators' measurement axes have been evaluated to determine the alignment parameters of the cube and the autocollimators. For this purpose, the slopes of the linear fits (straight lines) were calculated.

For the calibration grid regarded, the following alignment parameters have been determined with the relations given by equations (4) and (5) (all values in arcsec):

Cube	Autocollimator to be calibrated, AC_0	Horizontal reference autocollimator, AC_1	Vertical reference autocollimator, AC_2
W_α=3.7	$AC_{0\alpha}$=-53.0	$AC_{1\alpha}$=-1.0	$AC_{2\alpha}$=3.4
W_β=25.3	$AC_{0\beta}$=24.7	$AC_{1\beta}$=23.2	$AC_{2\beta}$=24.8
W_γ=46.1	$AC_{0\gamma}$=45.9	$AC_{1\gamma}$=30.9	$AC_{2\gamma}$=-76.2

5.3 Obtaining the tilting angles of the cube

All autocollimator measurement values are functions of the alignment parameters and the tilting angles of the cube (φ_y, φ_z). After the determination of the alignment parameters, their impact on the measurement values of the autocollimators can be taken into account and the cube's rotational angles determined. This is realised by an optimisation procedure.

As an illustration, a single measurement position with φ_y and φ_z, the tilting angles of the tilting unit, is considered. The actual measurement values of the reference autocollimators are denoted by $\tilde{H}_1$, $\tilde{V}_1$, $\tilde{H}_2$ and $\tilde{V}_2$. By using the polynomial equations (3), four functions are defined: $H_1(\varphi_y, \varphi_z)$, $V_1(\varphi_y, \varphi_z)$, $H_2(\varphi_y, \varphi_z)$ and $V_2(\varphi_y, \varphi_z)$ with φ_y and φ_z as variables, and the predetermined alignment parameters are inserted as constant parameters.

For the optimisation procedure, a quality measure is defined by

$$\Delta_{QM}(\varphi_y, \varphi_z) = \sum_{i=1}^{2} (|H_i(\varphi_y, \varphi_z) - \tilde{H}_i|^2 + |V_i(\varphi_y, \varphi_z) - \tilde{V}_i|^2) \quad (7)$$

It is minimised to obtain the best-fit estimates of the angles φ_y and φ_z:

The uncertainties of the best-fit angles are influenced by the measurement uncertainties of the autocollimators, including the limited repeatability of the measurements, and the uncertainties of the determination of the alignment parameters. The optimisation process is performed for all measurement positions of the calibration grid to obtain the respective tilting angles of the cube.

To visualise the effect of the alignment parameters on the best-fit tilting angles, their determination was performed twice. Once, without regarding the component alignment and, the other time, by considering the predetermined alignment parameters. The difference between both approaches is shown in Figure 7. The arrows express the differences between the corrected and uncorrected best-fit angles.

5.4 Spatial angle calibration results and comparison of plane angle calibrations

The last step in the spatial angle calibration process is the calculation of the expected measurement values of the

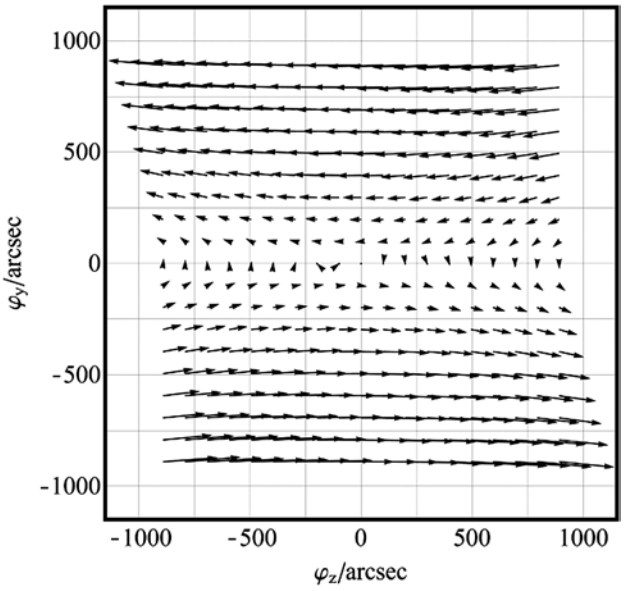

Figure 7: Vector representation of the differences between the corrected and the uncorrected best-fit tilting angles of the cube. The origins of the arrows correspond to the corrected angular values. The angle differences are given by the lengths of the arrows, scaled by a factor of 1500. The angle difference at the tilting unit's 'zero' position (φ_y=φ_z=0) has been subtracted from all differences. The maximum of the magnitude of the differences is 0.17 arcsec.

autocollimator to be calibrated by using the polynomial equations with the alignment parameters of the autocollimator and the best-fit tilting angles of the cube, φ_y and φ_z, which have been determined by the optimisation algorithm. The actual values, $\tilde{H}_0$ and $\tilde{V}_0$, are compared with the calculated measurement values of the autocollimator, H_0 and V_0, for each measurement position. The angle deviations are given by $\delta H_0(\varphi_y, \varphi_z)$ and $\delta V_0(\varphi_y, \varphi_z)$, where $\delta H_0(0, 0)$=$\delta V_0(0, 0)$=0 is valid, all angle deviations are regarded with respect to this definition.

5.4.1 19×19 calibration grid

Figure 8 shows the results of the spatial angle autocollimator calibration with 19×19 data points. Figure 8A presents calibration results without considering the alignment of the components. Figure 8B presents the calibration results with all corrections applied.

5.4.2 37×37 calibration grid

In Figure 9, the results of the spatial angle autocollimator calibration with 37×37 data points are shown. Notice the periodic angle deviations, which are specific for the examined autocollimator to be calibrated. They appear on smaller angular scales and, therefore, cannot be identified in the 19×19 pattern with its 150 arcsec step size.

5.5 Comparison with plane angle calibrations

The angular positions of the spatial angle calibration of the autocollimator, which correspond to the positions of

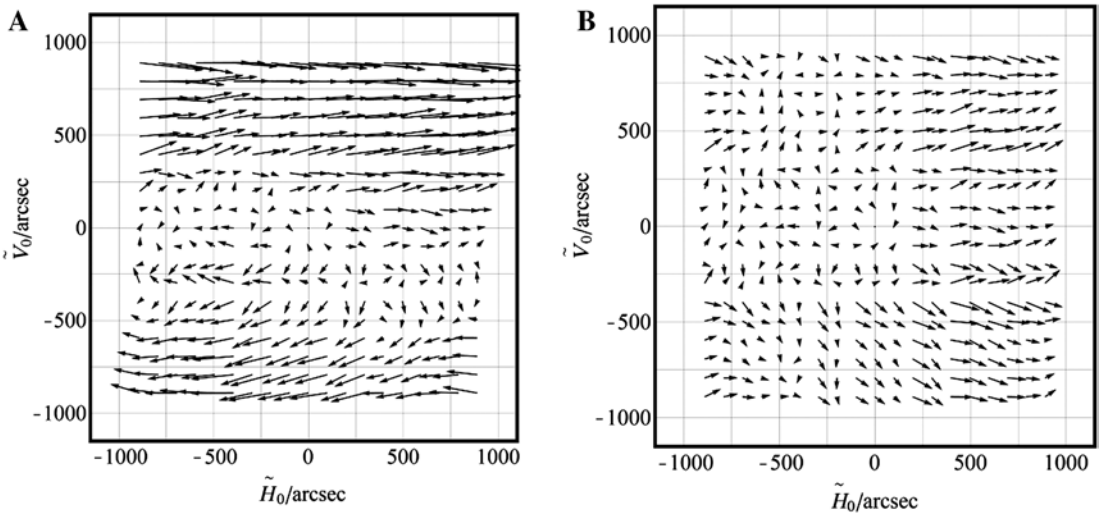

Figure 8: Results of the spatial angle calibration of an autocollimator with a grid of 19×19 measurement positions. The arrows represent the measurement deviations of the autocollimator, scaled by a factor of 1000. Their origins correspond to the measurement values of the autocollimator ($\tilde{H}_0$ and $\tilde{V}_0$). In the figure, (A) shows the calculated angle deviations of the autocollimator when no corrections regarding the component alignment and the non-orthogonalities have been applied, (B) shows the angle deviations with all corrections considered.

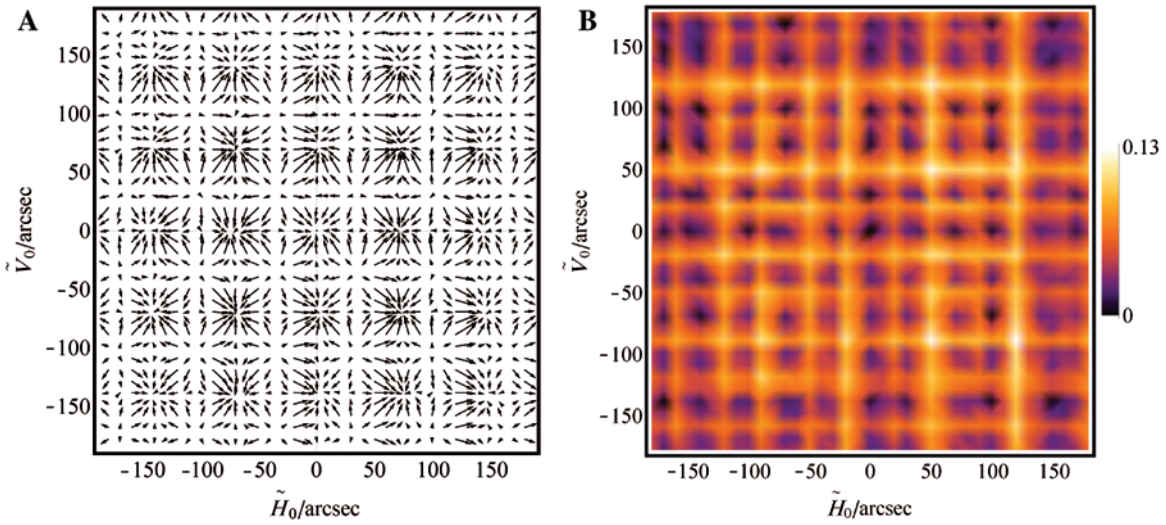

Figure 9: Results of the spatial angle calibration of an autocollimator for a 37×37 calibration grid. (A) Vector representation of the angle deviations (scaling factor: 175) of the autocollimator. (B) Heat map representation of the magnitude of the angle deviations. Owing to the small step size (10 arcsec) of the calibration grid compared to the 37×37 grid, the angle deviations with a period of approximately 70 arcsec are clearly resolved for both measurement axes of the autocollimator.

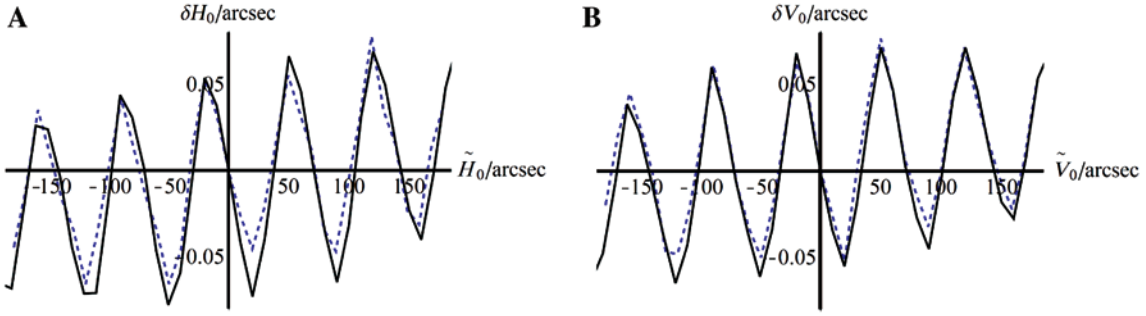

Figure 10: Comparison between the results of a conventional plane angle calibration of the autocollimator to be calibrated with the WMT 220 (black) and calibration data, which has been extracted from the 37×37 calibration grid obtained with the SAAC (blue, dashed). The selected measurement positions correspond to plane-angle measurements in the direction of the autocollimator's horizontal measurement axis (A) and vertical measurement axis (B). The step size of the spatial angle calibration grid is 10 arcsec.

the conventional (plane angle) calibration of its measurement axes ($\tilde{H}_0 \approx 0$ for the calibration of the autocollimator's vertical measurement axis, $\tilde{V}_0 \approx 0$ for the calibration of the horizontal measurement axis) have been extracted from the 37×37 calibration grid. They have been compared with the results of calibrations of the same autocollimator, which have been performed with the WMT 220, the primary angle standard of PTB. The results are shown in Figure 10.

The standard deviation of the differences between the conventional plane angle calibrations with the WMT 220 and the plane angle calibrations obtained with the SAAC, which have been extracted from the spatial angle calibration grid is 0.012 arcsec for the horizontal measurement axis and 0.007 arcsec for the vertical measurement axis of the autocollimator. The results of this comparison demonstrate the fundamental functionality of the SAAC regarding the stability, the positioning, the data acquisition, the implemented algorithms, and the evaluation of the measurements.

6 Conclusion and outlook

The test measurements with the SAAC prove the proper functioning of the system, including the measurement strategies and the alignment evaluation and correction methods, which we developed. The measurements include the first traceable calibration of an autocollimator

with both of its axes engaged simultaneously, which has been performed worldwide.

On the basis of the knowledge gained during the testing phase, the SAAC will be commissioned for regular operation. Our next steps will include evaluating the calibration uncertainty of the system and finding suitable sets of calibration parameters, regarding the calibration grid, step sizes and the number of repeat measurements. With the current setup, autocollimator calibrations at distances up to 1.5 m are feasible but are limited to static measurements. As the relative angular motion between the reflector cube and the linear stage during its movement is unknown, the calibrations at different distances are independent from each other. An interferometer will be integrated to measure those angles and, therefore, to enable the autocollimator calibrations at various distances to be connected. This allows the convenient characterising of distance-dependent effects on the autocollimator's angle measurements.

The provision of spatial angle calibrations of autocollimators at distances of up to 1.5 m by PTB's SAAC will be important in several ways. Autocollimator manufacturers will be able to improve their products by minimising cross-talk between the measuring axes and distance-dependent influences. Autocollimator users, especially users of deflectometric profilometers at synchrotrons, XFEL and NMI, will be able to benefit from the new calibration capabilities. Through these users, the traceable calibration of interferometers by the use of optical flatness standards (at NMI) and the manufacturing of beam-shaping optics for synchrotrons and XFEL applications can be improved.

Acknowledgments: Part of this research was undertaken within the European Metrology Research Programme (EMRP) Joint Research Project (JRP) SIB 58 Angle Metrology. The EMRP is jointly funded by the EMRP participating countries within the European Association of National Metrology Institutes (EURAMET) and the European Union.

Appendix

Method for the determination of the non-orthogonalities of the rotational axes of the tilting unit and the measurement axes of the autocollimator

The non-orthogonalities in this illustration are strongly exaggerated. The autocollimator's horizontal and vertical measurement directions are regarded as seen from the autocollimator standing upright (roll angle adjustment: 0°). They are co-rotated with the autocollimator. For the presentation of this method, the roll angle adjustments of the autocollimator are assumed to be ideal. See the note below regarding this constraint.

First roll angle adjustment: 0°

The autocollimator is adjusted as depicted in Figure 11: The reticle of the vertical measurement axis (V-Rtc, red line) is aligned parallel to the horizontal deflection direction of the reflected beam (H-Dfl, dashed line). For a horizontal tilting of the mirror, the autocollimator measures the deflection angle of the beam (along the H-Dfl line) with its horizontal CCD (H-CCD, thin black line), while the

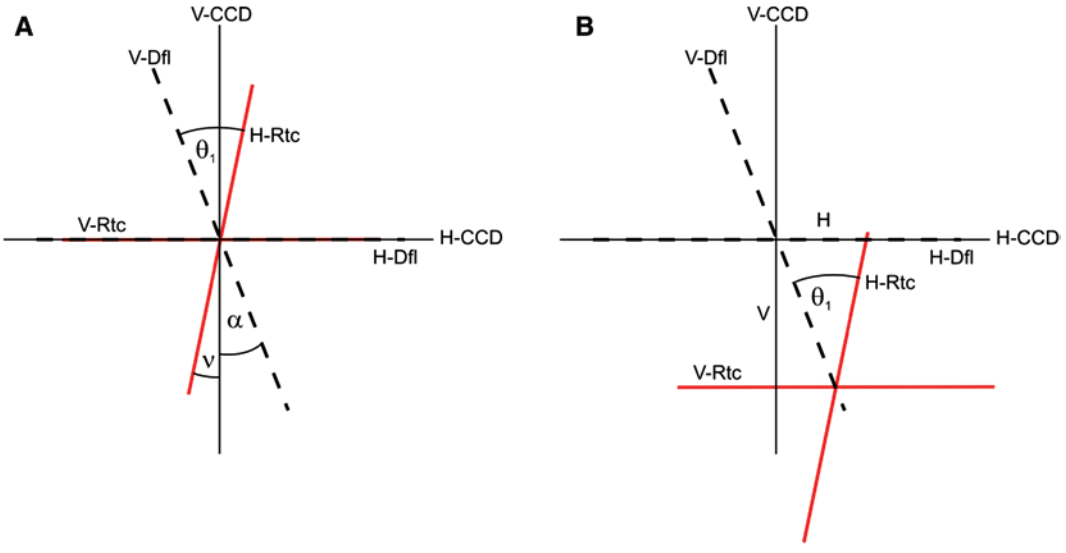

Figure 11: (A) shows the first autocollimator adjustment (roll angle 0°). Dfl: deflection directions of the reflected beam; Rtc: reticles; CCD: CCD lines; α: non-orthogonality of the rotational axes of the tilting unit; ν: non-orthogonality of the reticles; $\theta_1=\alpha+\nu$. (B) shows the effect of the vertical tilting of the mirror. Horizontal (*H*) and vertical (*V*) angles are measured.

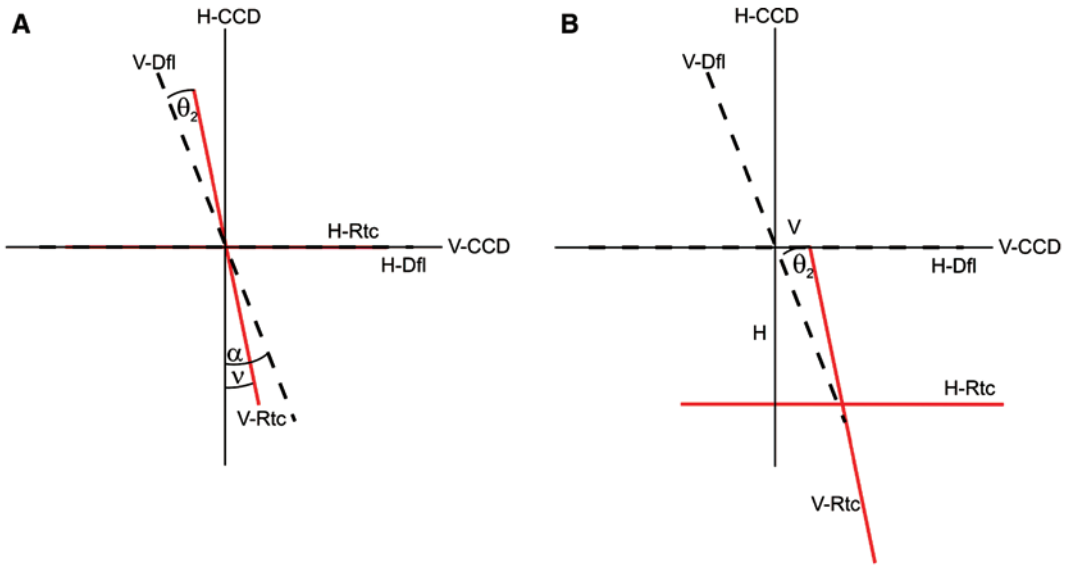

Figure 12: (A) shows the second autocollimator adjustment (roll angle 90°). The horizontal measurement value is zero for a horizontal tilting of the mirror. Here, $\theta_2=\nu-\alpha$ is valid. (B) shows the effect of the vertical tilting of the mirror. Again, horizontal (*H*) and vertical (*V*) angles are measured.

vertical measurement value is constantly zero. When the mirror is tilted vertically, not only the vertical deflection angle (along the V-Dfl line) is measured by the autocollimator's vertical CCD (V-CCD) but also the horizontal measurement value is =0 due to the non-orthogonalities of the reticles (ν) and the rotational axes of the tilting unit (α).

For this roll angle adjustment, the angle θ_1 is calculated by evaluating the measurement values of the autocollimator (using the approximation $\tan\theta_1\approx\sin\theta_1\approx\theta_1$ for small angles θ_1):

$$\frac{\partial H}{\partial V}\approx\theta_1=\nu+\alpha \tag{A.1}$$

where H is the horizontal, and V is the vertical measurement value of the autocollimator.

A note on the experimental application of the method: A residual misalignment (non-parallelism) between the reticle of the autocollimator's vertical measurement axis (V-Rtc) and the horizontal deflection direction of the tilting system (H-Dfl) can be evaluated by the use of autocollimator measurements performed during the horizontal deflection of the tilting system. The resulting angle between V-Rtc and H-Dfl can then be used for correcting the angle θ_1 by adding or subtracting it.

Second roll angle adjustment: 90°

For the second roll angle adjustment of the autocollimator, it is rotated by approximately 90° (Figure 12) with respect to its optical axis to align the reticle of its horizontal measurement axis (H-Rtc) parallel to the horizontal deflection direction of the reflected beam (H-Dfl). For a horizontal tilting of the mirror, the autocollimator measures the deflection angle of the beam (along the H-Dfl line) with its vertical CCD (V-CCD), while the horizontal measurement value is constantly zero. The mirror is tilted vertically again. The horizontal CCD (H-CCD) measures the vertical deflection (along the V-Dfl line). The vertical measurement value is ≠0, due to the non-orthogonalities.

For the second roll angle adjustment, the angle θ_2 is given by:

$$\frac{\partial V}{\partial H}\approx\theta_2=\nu-\alpha \tag{A.2}$$

With equation (A.1) and (A.2) one obtains

$$\frac{\theta_1+\theta_2}{2}=\nu \tag{A.3}$$

$$\frac{\theta_1-\theta_2}{2}=\alpha \tag{A.4}$$

To be compliant with the parameter definitions of the SAAC, $\alpha=r_{y\alpha}$ and $\nu=V_{0\nu}$ are valid.

References

[1] H. Lammert, F. Senf and M. Berger, Proc. SPIE 3152, 168–179 (1997).
[2] R. D. Geckeler and A. Just, Proc. SPIE 6704, 670407-1 (2007).

[3] R. D. Geckeler, A. Just, M. Krause and V. V. Yashchuk Nucl. Instrum. Methods Phys. Res. Sect. A 616, 140 (2010).
[4] F. Siewert, H. Lammert and T. Zeschke, in 'Modern Developments in X-Ray and Neutron Optics', Eds. By A. Erko, M. Idir, T. Krist and A.G. Michette (Springer, Berlin, 2008) pp. 193–200.
[5] V. V. Yashchuk, S. Barbera, E. E. Domninga, J. L. Kirschmana, G. Y. Morrisona, et al., Nucl. Instrum. Methods Phys. Res. Sect. A 616, 212 (2010).
[6] G. Ehret, M. Schulz, M. Stavridis and C. Elster, Meas. Sci. Technol. 23, 094007 (2012).
[7] F. Siewert, J. Buchheim, S. Boutet, G. J. Williams, P. A. Montanez, et al., Opt. Express 20, 4 (2012).
[8] A. Just, M. Krause, R. Probst and R. Wittekopf, Metrologia 40, 288 (2003).
[9] R. D. Geckeler and A. Just, Proc. SPIE 7077, 70770B (2008).
[10] R. Probst, G. Fuetterer, J. Illemann, J. Mokros, P.K. Lui, et al. Proc. 7th Int. Conf. Euspen 2, 121 (2007).
[11] R. Probst, R. Wittekopf, M. Krause, H. Dangschat and A. Ernst, Meas. Sci. Technol. 9, 1059 (1998).
[12] R. D. Geckeler, O. Kranz, A. Just and M. Krause, Adv. Opt. Technol. 1, 427 (2012).
[13] http://www.moeller-wedel-optical.com/en/produkte/electronic-autocollimators/p-elcomat-3000.html (accessed 2014-11-13).
[14] R. D. Geckeler and A. Just, Meas. Sci. Technol. 25, 105009 (2014).
[15] O. Kranz, R. D. Geckeler, A. Just and M. Krause, Proc. SPIE 8789, 87890D (2013).
[16] R. D. Geckeler, Meas. Sci. Technol. 18, 115 (2007).
[17] S. K. Barber, R. D. Geckeler, V. V. Yashchuk, M. V. Gubarev, J. Buchheim, et al., Opt. Eng. 50, 073602 (2011).
[18] P. J. Sim, in 'Modern Techniques in Metrology', Ed. By P. Hewitt (World Scientific, Singapore, 1984) pp. 102–112.
[19] International vocabulary of metrology – Basic and general concepts and associated terms (VIM) JCGM 200:2012 http://www.bipm.org/en/publications/guides/vim.html (accessed 2014-11-13).

Oliver Kranz
Physikalisch-Technische Bundesanstalt (PTB), Bundesallee 100, D-38116 Braunschweig, Germany,
oliver.kranz@ptb.de

Oliver Kranz received his university degree (diploma) in physics from the Leibniz Universität, Hannover, Germany, in 2009. He works as a PhD student in the Length and Angle Graduations Group at PTB. His work focuses on the characterisation of autocollimators in experiments, ray-tracing simulations and mathematical modelling. In addition, he is involved in PTB's Spatial Angle Autocollimator Calibrator (SAAC), a novel calibration device for autocollimators.

Ralf D. Geckeler
Physikalisch-Technische Bundesanstalt (PTB), Bundesallee 100, D-38116 Braunschweig, Germany

Ralf D. Geckeler received his PhD from the Eberhard-Karls University, Tübingen, Germany. He heads the Length and Angle Graduations Group at PTB, the national metrology institute of Germany. His research focuses on angle measuring devices, such as autocollimators and angle encoders, in international collaboration with industry and research institutes. Current topics include the improvement of autocollimator performance and calibration, the advancement of angle metrology for the characterisation of beamline optics at synchrotron and FEL facilities worldwide, and the development of novel methods and advanced mathematical algorithms for the calibration of angle measuring devices.

Andreas Just
Physikalisch-Technische Bundesanstalt (PTB), Bundesallee 100, D-38116 Braunschweig, Germany

Andreas Just received his university degree (diploma) from the Technical University 'Otto von Guericke', Magdeburg, Germany, in 1986. He is a member of the Length and Angle Graduations Group at PTB. His work focuses on the calibration of angle standards and instruments, such as autocollimators, and the development of new calibration methods.

Michael Krause
Physikalisch-Technische Bundesanstalt (PTB), Bundesallee 100, D-38116 Braunschweig, Germany

Michael Krause received his university degree (diploma) from the University of Applied Sciences, Lübeck, Germany, in 1987. He is a member of the Length and Angle Graduations Group at PTB. His work focuses on angle encoder calibrations and the development of software for analyses of self- and cross-calibration data from these encoders, including PTB's primary angle standard WMT 220 for the SI unit 'radian'. He is also responsible for the automatisation of calibration set-ups.

Wolfgang Osten
Institut für Technische Optik (ITO)
Universität Stuttgart, Pfaffenwaldring 9
D-70569 Stuttgart, Germany

Wolfgang Osten received the Diploma in Physics from the Friedrich-Schiller-University Jena in 1979 and in 1983 the PhD degree from the Martin-Luther-University Halle-Wittenberg for his thesis in the field of holographic interferometry. From 1984 to 1991 he was employed at the Central Institute of Cybernetics and Information Processes in Berlin making investigations in digital image processing and computervision. In 1991 he joined the Bremen Institute of Applied Beam Technology (BIAS) to establish the Department Optical 3D-Metrology. Since September 2002 he has been a full professor at the University of Stuttgart and director of the Institute for Applied Optics. His research work is focused on new concepts for industrial inspection and metrology by combining modern principles of optical metrology, sensor technology and image processing. Special attention is directed to the development of resolution enhanced technologies for the investigation of micro and nano structures.